Pulsed laser deposition of thick $BaHfO_3$-doped $YBa_2Cu_30_{7-\delta}$ films on highly alloyed textured Ni-W tapes

To cite this article: M Sieger *et al* 2014 *J. Phys.: Conf. Ser.* **507** 022032

Journal of Physics: Conference Series **507** (2014) 022032 doi:10.1088/1742-6596/507/2/022032

Pulsed laser deposition of thick $BaHfO_3$-doped $YBa_2Cu_3O_{7-\delta}$ films on highly alloyed textured Ni-W tapes

M Sieger, J Hänisch, K Iida, U Gaitzsch, C Rodig, L Schultz, B Holzapfel, R Hühne

Institute for Metallic Materials, IFW Dresden, PO Box 270116, 01171 Dresden, Germany

m.sieger@ifw-dresden.de

Abstract. $YBa_2Cu_3O_{7-\delta}$ (YBCO) films with a thickness of up to 3 µm containing nano-sized $BaHfO_3$ (BHO) have been grown on Y_2O_3/Y-stabilized ZrO_2/CeO_2 buffered Ni-9at% W tapes by pulsed laser deposition (PLD). Structural characterization by means of X-ray diffraction confirmed that the YBCO layer grew epitaxial. A superconducting transition temperature T_c of about 89 K with a transition width of 1 K was determined, decreasing with increasing BHO content. Critical current density in self-field and at 0.3 T increased with increasing dopant level.

1. INTRODUCTION

The high-temperature superconductor $YBa_2Cu_3O_{7-\delta}$ (YBCO)[1] might be used for technical applications such as superconducting transmission cables, motors and electrical power components due to its superior current transport capability in high magnetic fields.[2] The critical current I_c can be increased by improving the critical current density J_c for a constant film thickness t or by increasing t for a constant J_c. Artificial pinning centres as nanoparticles like $BaHfO_3$ (BHO)[3,4] form effective immobilization points for magnetic flux lines,[5] thereby increasing $J_c(\mu_0 H)$. One of the main approaches to realize long length coated conductors is to use Ni-W tapes with a strong cube texture, formed by heavy cold rolling and annealing.[6] Recently, Ni-9at% W (Ni9W) tapes were realized, which are non-magnetic at 77 K and therefore reduce AC losses of the conductors.[7] A suitable buffer layer architecture as for example Y_2O_3/Y-stabilized ZrO_2 (YSZ)/CeO_2[8] ensures epitaxial growth to prevent high-angle grain boundaries, which are highly detrimental to the transport current.[9] Here, we demonstrate thick YBCO films grown on Ni9W. Furthermore, BHO pinning centres were incorporated into the YBCO matrix using PLD targets from mixed powders to increase the current transport capability in magnetic fields.

2. EXPERIMENTAL DETAILS

A *Lambda Physics LPX305i* KrF excimer laser (λ = 248 nm, t_{pulse} = 25 ns) with an energy density of 1.6 J/cm² at the surface of the PLD target was used to grow superconducting films on 10 mm × 10 mm × 1 mm single crystalline (100) oriented $SrTiO_3$ (STO) substrates as well as on 10 mm × 10 mm × 80 µm sized biaxially textured Ni9W tapes with a Y_2O_3/YSZ/CeO_2 buffer layer stack on top. The details of the tape preparation and buffer layer deposition may be found in Ref. [8]. An oxygen partial pressure of 0.4 mbar was maintained during the deposition process. The deposition temperature was set to 810°C for STO substrates and to 830°C for Ni9W tapes, which were found as optimum conditions for high critical temperature and current density in previous experiments. Undoped as well as 2, 4 and 6 mol% BHO-doped YBCO films were deposited from PLD targets which were prepared from mixed powders by a conventional solid state reaction. In-situ oxygen loading of the YBCO films took place in 400 mbar O_2 during cooling at 20 K min^{-1} in order to obtain superconducting YBCO.

The surface morphology was studied using a *Philips XL 20* scanning electron microscope, and the film thickness was measured on cross sectional cuts prepared by a focused gallium ion beam in a *FEI Helios 600i*. The crystal structure was determined in a *Bruker D8 Advance* X-ray diffractometer in Θ-2Θ geometry. Pole figures were taken by a *Philips X´Pert PW3040* on the YBCO (102) and BHO (110) planes. Superconducting properties, i.e. critical temperature $T_{c,50}$ (measured at midpoint of transition), the transition width ΔT_c, and the critical current densities J_c^{sf} and $J_c^{0.3T}$ (J_c in self-field and in a magnetic field of 0.3 T parallel *c*), were measured inductively.

3. RESULTS AND DISCUSSION

3.1. Growth of thick YBCO films on STO single crystalline substrates

The X-ray diffraction patterns of three different samples on STO are shown in figure 1(a). The deposition frequency was increased with increasing film thickness to keep the growth time nearly constant. All samples show strong (00ℓ) YBCO peaks, which is a clear sign of *c*-axis oriented growth on the STO substrates. Additional peaks are assigned as Y_2O_3 inclusions originating from excess yttrium in the target. The thickest sample shows additional *a*-axis oriented YBCO grains due to the presence of (*h*00) reflections. The (102) YBCO pole figures for the 1 µm and 3 µm thick films are given in figures 1(b) and 1(c). Whereas an undisturbed epitaxial growth was observed for the 1 µm thick film, a significant amount of *a*-axis oriented grains is present in the 3 µm thick film, which is visible at an angle ψ of approximately 33°. It should be noted that the *a*-axis oriented growth was prevented in a 3 µm thick film by employing a laser frequency of 10 Hz.

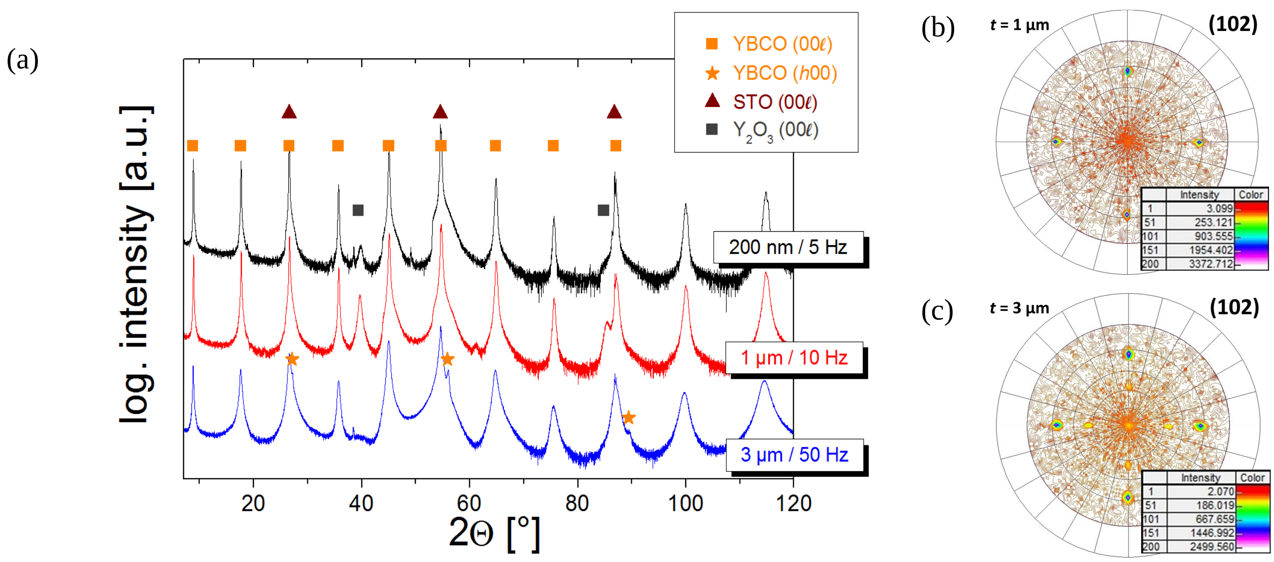

Figure 1: Structural characterization of undoped YBCO samples on STO having different thicknesses: X-ray diffraction pattern (a); YBCO (102) pole figure of a 1 µm (b) and 3 µm (c) thick layer

Table 1 summarizes the superconducting properties for this sample series. The critical temperature $T_{c,50}$ of the 1 µm thick sample is slightly increased compared to the 0.5 µm thin film. However, the critical current density J_c^{sf} is strongly reduced from 2.7 MA/cm² (0.5 µm) to 1.8 MA/cm² (1 µm). The

3 µm thick sample shows a significant drop in both, T_c and J_c^{sf}, which may have several reasons. On the one hand, a relatively long *c*-axis, compared to the other samples, indicates a lower oxygen content leading to a reduced critical temperature. On the other hand, high-angle grain boundaries due to *a*-axis oriented grains might be responsible for lower J_c values. A change to rougher morphologies with increasing thickness may also contribute to the J_c drop.[10]

Table 1: $T_{c,50}$ and critical current density in self-field, J_c^{sf}, at liquid nitrogen temperature for undoped YBCO samples with different thicknesses grown on STO

thickness	f_{Dep}	$T_{c,50}$	ΔT_c	J_c^{sf}
[µm]	**[Hz]**	**[K]**	**[K]**	**[MA/cm²]**
0.5	5	90.9	1.2	2.71 ± 0.12
1	10	92.4	1.0	1.83 ± 0.62
3	50	86.4	1.8	0.38 ± 0.11

3.2. BHO-doped YBCO samples on highly alloyed textured metal tapes

Thicker YBCO layers were grown on Ni9W in the next step, using a laser repetition rate of 10 Hz. Figure 2(a) shows a top view of a 1.8 µm thick YBCO film on a buffered Ni9W tape. The grain structure, which is transferred from metal tape via buffer layers, is clearly visible. Only a small number of Ni recrystallization twins, which are detrimental to *c*-axis aligned growth of YBCO, are present. The higher magnification view (figure 2(b)) shows the small YBCO islands which coalesce during film growth.[11] The cross sectional view in figure 2(c) shows the complete layer architecture with the metal tape, the threefold buffer layer stack and YBCO. Additionally, nickel oxide (NiO) and nickel tungsten oxide ($NiWO_4$) are found at the tape/buffer interface.

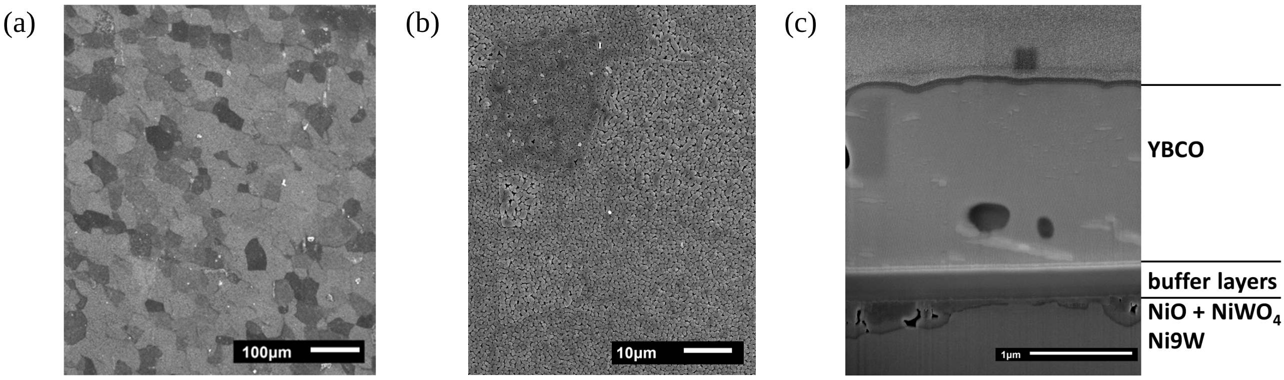

Figure 2: Surface morphology of undoped YBCO on biaxially textured Ni9W tape: top view (a), higher magnification (b), lateral view of a cross section (c)

The epitaxial growth on the biaxially textured metal tape is proven by the presence of (00ℓ) peaks of the buffer layers and YBCO in figure 3(a) as well as by pole figure measurements. The YBCO (102) peaks in the pole figure in figure 3(b) show the typical broadening, already present in the Ni9W substrate. The average (4 peaks) in-plane full width at half maximum is 6.2° for YBCO, which is similar to the value of 6.4° for the substrate. Figure 3(c) shows that BHO is incorporated into the films with a biaxial, cube-on-cube relationship. The additional strong peaks at $\Psi = 55°$ arise from the Y_2O_3 (222) planes, which have almost the same 2Θ value as the BHO (110) plane.

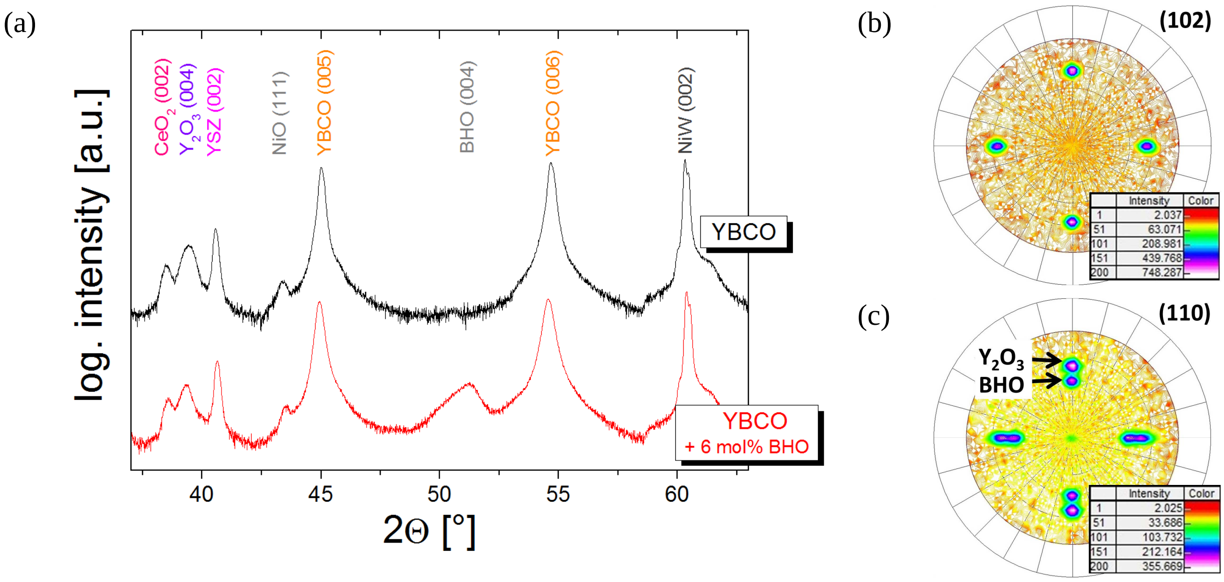

Figure 3: Structural characterization of YBCO samples on Ni9W: X-ray diffraction pattern of 1.8 µm thick undoped and 6 mol% BHO-doped YBCO (a); with respective YBCO (102) pole figure (b); and BHO (110) pole figure (c)

Whereas the critical temperature of the YBCO films on Ni9W decreases slightly with increasing BHO concentration, the critical current density increases in self-field and even more pronounced at 0.3 T applied parallel to the *c*-axis of the films (see table 2). Pinning effects in higher fields will be investigated by detailed transport J_c studies in the near future.

Table 2: Critical temperature and critical current density of 1.8 µm thick undoped and BHO-doped YBCO samples on biaxially textured Ni9W tapes deposited with a frequency of 10 Hz

BHO content	$T_{c,50}$	ΔT_c	J_c^{sf}	$J_c^{0.3T\|\|c}$
[mol%]	[K]	[K]	[MA/cm²]	[MA/cm²]
0	89.1	1.0	0.38 ± 0.01	0.15 ± 0.01
2	88.1	0.8	0.33 ± 0.01	0.19 ± 0.01
4	88.4	0.7	0.60 ± 0.04	0.32 ± 0.01
6	87.7	0.9	0.73 ± 0.02	0.33 ± 0.02

The authors gratefully thank J. Scheiter, U. Fiedler and M. Kühnel for technical assistance and acknowledge the financial support from EUROTAPES, a collaborative project funded by the European Community's Seven Framework Programme (FP7 / 2007 - 2013) under Grant Agreement no. 280432.

References

[1] Wu M *et al* 1987 *Phys. Rev. Lett.* **58** 908-910
[2] Foltyn S *et al* 2007 *Nat. Mater.* **6** 631-642
[3] Hänisch J *et al* 2006 *Supercond. Sci. Technol.* **19** 534-540
[4] Engel S *et al* 2000 *Appl. Phys. Lett.* **90** 102505
[5] Matsushita T 2000 *Supercond. Sci. Technol.* **13** 730-737
[6] Eickemeyer J *et al* 2010 *Supercond. Sci. Technol.* **23** 085012
[7] Gaitzsch U *et al* 2013 *Supercond. Sci. Technol.* **26** 085024
[8] Hühne R *et al* 2007 *Supercond. Sci. Technol.* **20** 709-714
[9] Hilgenkamp H and Mannhart J 2002 *Rev. Mod. Phys.* **74** 485-549
[10] Foltyn S *et al* 1999 *Appl. Phys. Lett.* **75** 3692-3694
[11] Hühne R *et al* 2010 *Supercond. Sci. Technol.* **23** 034015

Corrigendum: Pulsed laser deposition of thick $BaHfO_3$-doped $YBa_2Cu_3O_{7-\delta}$ films on highly alloyed textured Ni-W tapes

M Sieger, J Hänisch, K Iida, U Gaitzsch, C Rodig, L Schultz, B Holzapfel, R Hühne

Institute for Metallic Materials, IFW Dresden, PO Box 270116, 01171 Dresden, Germany

m.sieger@ifw-dresden.de

CORRIGENDUM TO: *JPCS* **507** (2014) 022032

The presented BHO doped YBCO films on STO turned out to have a higher thickness than we expected by earlier experiments under similar conditions (pulse number, oxygen pressure, substrate temperature, laser energy). Some inductive values of the critical current density had to be recalculated and the measured thicknesses are included in the tables.

Table 1: $T_{c,50}$ and critical current density in self-field, J_c^{sf}, at liquid nitrogen temperature for undoped YBCO samples with different thicknesses grown on STO

thickness	f_{Dep}	$T_{c,50}$	ΔT_c	J_c^{sf}
[µm]	[Hz]	[K]	[K]	[MA/cm²]
0.5	5	90.9	1.2	2.71 ± 0.12
2.0	10	92.4	1.0	0.74 ± 0.15
3.3	50	86.4	1.8	0.35 ± 0.12

Table 2: Critical temperature and critical current density of ~2 µm thick undoped and BHO-doped YBCO samples on biaxially textured Ni9W tapes deposited with a frequency of 10 Hz

thickness	BHO content	$T_{c,50}$	ΔT_c	J_c^{sf}	$J_c^{0.3T\|\|c}$
[µm]	[mol%]	[K]	[K]	[MA/cm²]	[MA/cm²]
1.8	0	89.1	1.0	0.38 ± 0.01	0.15 ± 0.01
2.1	2	88.1	0.8	0.33 ± 0.01	0.19 ± 0.01
2.0	4	88.4	0.7	0.60 ± 0.04	0.32 ± 0.01
1.8	6	87.7	0.9	0.73 ± 0.02	0.33 ± 0.02

Thereby some numbers in section 3.1 change accordingly. The conclusion is not altered by this correction.